PM20

XAFS study for formation mechanism of nanoparticles in supercritical water

Akira Yoko[a],*, Yoshito Oshima[b], Tadafumi Adschiri[a,c,d]

a. WPI - Advanced Institute for Materials Research (WPI-AIMR), Tohoku University, 2-1-1 Katahira, Aoba-ku, Sendai, Miyagi 980-8577, Japan

b. Department of Environment Systems, Graduate School of Frontier Sciences, The University of Tokyo, Kashiwanoha 5-1-5, Kashiwa, Chiba 277-8563, Japan

c. New Industry Creation Hatchery Center, Tohoku University, Japan

d. Institute of Multidisciplinary Research for Advanced Materials, Tohoku University, Japan

* akira.yoko.c7@tohoku.ac.jp

ABSTRACT

Supercritical hydrothermal synthesis is expected as a methodology for fabricating new nanomaterials. High super-saturation degree in supercritical water enables rapid formation of nanostructures, and rapid crystallization can produce materials of characteristic composition and structure. Formation of composite oxide in supercritical water has been studied with *ex situ* and *in situ* methods. In the previous study, we observed the existence of the highly defective structure during the crystallization in the case of perovskite-type composite oxide.

In this study, perovskite-type composite oxides nanoparticles such as $BaZrO_3$ and $SrZrO_3$ were synthesized in supercritical water using a continuous flow reactor, and the nanoparticle formation at highly supersaturated environments was studied. Local structure of nanoparticles was focused, and characterized mainly by X-ray absorption fine structure (XAFS). In addition to the measurements of nanoparticles, a theoretical calculation was also conducted to study surface structure of nanoparticles.

Formation of highly defective structure which was observed in the previous studies was intensively investigated in terms of local structure. Increase in coordination number

and decrease in the Debye-Waller factor with an increase in residence time was observed by the XAFS measurements, which suggest the formation of highly defective structure and following uptake reaction filling the deficiency in supercritical water.

INTRODUCTION

Supercritical hydrothermal synthesis method [1] is a methodology for fabricating various kinds of nanoparticles with small size and narrow size distribution. One of the characteristic points of the technique is a rapid formation of nanostructures owing to the high super-saturation degree in supercritical water. Rapid crystallization can produce materials of characteristic composition and structure under non-equilibrium state [2,3], and supercritical hydrothermal method is promising for finding new nanomaterials. Also, fine-control of nanoparticles enables us to study nanostructures which are different from the bulk structure.

Not only single-component metal oxides but also composite oxides composed of multiple metal ions can be synthesized by the supercritical method. Non-equilibrium state and non-stoichiometric composition is an important aspect in the synthesis of composite oxides. We have studied perovskite-type composite oxides formation in supercritical water with *ex situ* [4,5] and *in situ* [6] methods and showed the existence of the highly defective structure of zirconate during the crystallization. Single particle analysis with TEM-EDX revealed that A-site ion, for example, Ba, is taken up into defective perovskite structure in supercritical water. Also, lattice expansion of the order of milliseconds caused by the ion uptake was detected by *in situ* synchrotron X-ray diffraction.

To elucidate such a characteristic deficient structure, X-ray absorption fine structure (XAFS) analysis is suitable. By use of XAFS technique, the local structure such as coordination number and coordination distance can be analyzed. In addition, the atomic selective analysis is possible with XAFS, which is impossible by other measurements such as diffraction. Moreover, non-crystalline or disordered structures frequently observed in nanoparticles are also measurable by XAFS.

In this study, *ex situ* study using XAFS was conducted for composite oxides formation of the order of seconds via time-resolved experiments with a continuous flow reactor. Perovskite-type composite oxide nanoparticles such as $BaZrO_3$ and $SrZrO_3$ were synthesized in supercritical water using a continuous flow reactor, and the nanoparticle structures formed at highly supersaturated environments as supercritical conditions were investigated. Local structure of nanoparticles formed in supercritical water was focused, and the XAFS measurements were mainly conducted for detailed

analysis of the local structure. In addition to the XAFS measurements of nanoparticles, theoretical calculation for nanostructure formation [7] was also conducted to study disordered structure of nanoparticles.

MATERIALS AND METHODS

Barium nitrate [$Ba(NO_3)_2$ (purchased from Kanto Chemical Co., Inc.)] and oxy-zirconium nitrate [$ZrO(NO_3)_2 \cdot 2H_2O$ (purchased from Kanto Chemical Co., Inc.)] were used as starting materials. Potassium hydroxide [KOH (purchased from Wako Pure Chemical Industries Ltd.)] was used as a base solution for tuning the pH. Nitric acid [HNO_3 (purchased from Wako Pure Chemical Industries Ltd.)] was used to neutralize the recovered solution. Distilled water (produced from RFD240HA; Advantec MFS, Inc.) was used in the preparation of the feed solution. An excess of Ba, relative to the amount of Zr (4 times), was used in the starting solutions to obtain mono-phase products following the previous study of $BaZrO_3$ formation [4]; otherwise, the ZrO_2 phase is also contained in products. For the XAFS measurements, micrometer order of ZrO_2 and $BaZrO_3$ (purchased from Sigma Aldorich) were used as references of the bulk crystal.

All experiments were performed using the continuous flow reactor. Starting solutions of barium and zirconium were simultaneously mixed with the base solution and heated distilled water, using a cross-shaped part (SUS316; inner diameter: 1.3 mm). The starting solution and base solution were introduced into the reactor at a flow rate of 10 g min^{-1}, and heated distilled water was introduced at 80 g min^{-1} using a non-pulsation pump (NP-KX-500; Nihon Seimitsu Co., Ltd.). The starting solution and the base solution were cooled just before the mixing point, to prevent warming of the starting solutions *via* conductive heat transfer before mixing. The flow rates set a Reynolds number (*Re*) of 4×10^4 at the reactor, just after mixing. Kawasaki *et al.* investigated the relationship between particle size and *Re*, and suggested that sufficient mixing was achieved at values of $Re \geq 4 \times 10^4$; at these values, the mixing conditions did not affect the particle size [8]. The temperature of the water was set at 400 °C at the point just before cooling. The pressure was set at 30 MPa using a back-pressure regulator (BP66-112865; Go Inc.). The residence time was set from 0.1-10.7 s by changing the reactor volume from the mixing point to the point just before the cooling. After cooling, an HNO_3 solution was introduced using a flow rate of 5 g min^{-1}, to reconcile the pH and prevent the formation of carbonate in the recovered dispersion.

The solid products were recovered *via* pressurized filtering using a nitrocellulose filter (VSWP14250; Merck Millipore Corporation, pore size: 0.025 μm), and were dried in a

vacuum oven at room temperature (ADP-31; Yamato Corporation). The recovered particles were analyzed as described as follows.

XAFS was conducted at BL01B1 of SPring-8, JASRI. For the Zr K edge spectra, Si (111) double-crystal monochromator was used, and for Ba K edge spectra, Si (311) double-crystal monochromator was used. Transmission method was applied, and pellet sample with BN binder was used for the measurements. X-rays intensity was measured by ionization chambers before (I_0) and after (I) the sample (70%-N_2 and 30%-Ar for I_0, 90%-Ar, and 10%-Kr for I). EXAFS data were analyzed by FEFF code. For the initial structures for the fitting, crystallographic information obtained by diffraction was used. As for the analysis, EXAFS frequency in *k* space, $\chi(k)$ written as follows was used.

$$\chi(\mathrm{k}) = {S_0}^2 \sum_j \frac{N_j \left|F_j(k)\right| \exp\left(-2k^2{\sigma_j}^2\right)}{k{r_j}^2} \sin\left(2kr_j + \emptyset_j(k)\right)$$

Here, coordination number, N_j, coordination distance, r_j, and Deby-Waller factor, ${\sigma_j}^2$, are the fitting parameters, and backscatter factor, $\left|F_j(k)\right|$ and phase shift, $\emptyset_j(k)$ were theoretically calculated by FEFF code. As can be seen in the equation, amplitude of $\chi(k)$ increase with an increase in coordination number or decrease in Debye-Waller factor, and frequency of $\chi(k)$ increase with an increase in coordination distance. As an index of the accuracy of the fitting, R-factor, as follows, was checked after fittings. Smaller R-factors indicate the high accuracy of the fittings, and R-factor < 0.1 was confirmed for all the samples in this study.

$$\mathrm{R-factor} = \sqrt{\frac{\sum_i \left({\chi_i}^{data}(k) - {\chi_i}^{fit}(k,[a])\right)^2}{\sum_i \left({\chi_i}^{data}(k)\right)^2}}$$

RESULTS

Local structure of highly deficient $BaZrO_3$ formed in supercritical water was analyzed by EXAFS. Figure 1 shows EXAFS frequency, radial structure function, and inverse Fourier transform function of Zr K edge for the bulk reference of $BaZrO_3$. The range of Fourier transform is 3-14 $Å^{-1}$, and fitting was conducted for radial distribution function in the range of 1.2-3.4 Å corresponding to first coordination, Zr-O and second coordination, Zr-Ba. Inverse Fourier transform was conducted for radial structure function in the range of 1.2-3.4 Å and as can be seen in Figure 1(C), the measured

frequency was well reproduced by the fitting, resulting in R-factor of 0.059. Figure 2 and Figure 3 shows EXAFS data for the nanoparticles synthesized in supercritical water with 0.1 s and 10.7 s, respectively. Fittings for both of the data were converged to the R-factor of 0.042 for 0.1 s and 0.037 for 10.7 s.

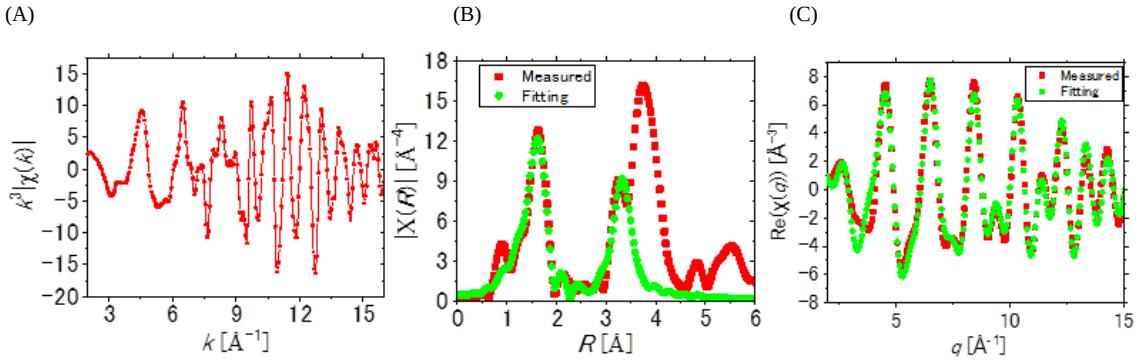

Figure 1. Zr K edge of the bulk reference sample. (A) EXAFS frequency, (B) radial distribution function with fitting for first and second coordination, and (C) real part of inverse Fourier transform of radial distribution function in the range of the fitting with R-factor, 0.059.

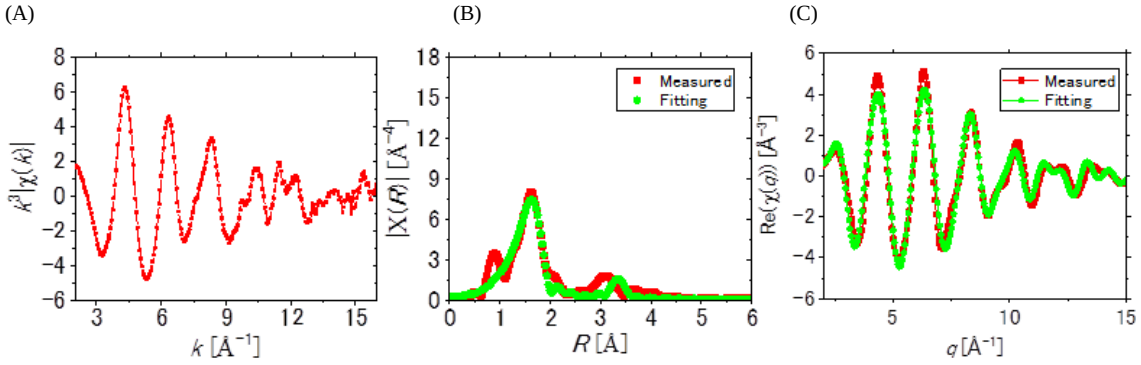

Figure 2. Zr K edge of nanoparticles synthesized in 0.1 s. (A) EXAFS frequency, (B) radial distribution function with fitting for first and second coordination, and (C) real part of inverse Fourier transform of radial distribution function in the range of fitting with R-factor, 0.042.

(A) (B) (C)

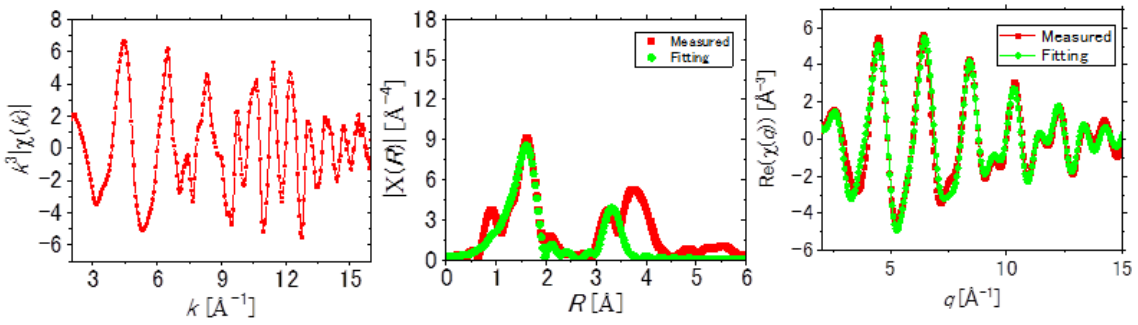

Figure 3. Zr K edge of nanoparticles synthesized in 10.7 s. (A) EXAFS frequency, (B) radial distribution function with fitting for first and second coordination, and (C) real part of inverse Fourier transform of radial distribution function in the range of fitting with R-factor, 0.037.

EXAFS of Ba K edge was also measured in the same way. Figure 4, Figure 5, and Figure 6 shows the bulk, nanoparticle synthesized in 0.5 s, and nanoparticles synthesized in 10.7 s (R-factor, bulk: 0.016, 0.5 s: 0.010, 10.7 s: 0.010). In the case of Ba K edge, the range of Fourier transform was set to 3-12 $Å^{-1}$, and fitting was conducted for radial structure function in the range of 1.4-4.0 Å, corresponding to first to third coordinations (Ba-O, Ba-Zr, and Ba-Ba). During the fitting of those EXAFS data, the ratio of the mean square displacement of each site calculated by first-principles molecular dynamics simulation was used as a constraint condition to obtain coordination number avoiding the correlation of coordination number and Debye-Waller factor.

(A) (B) (C)

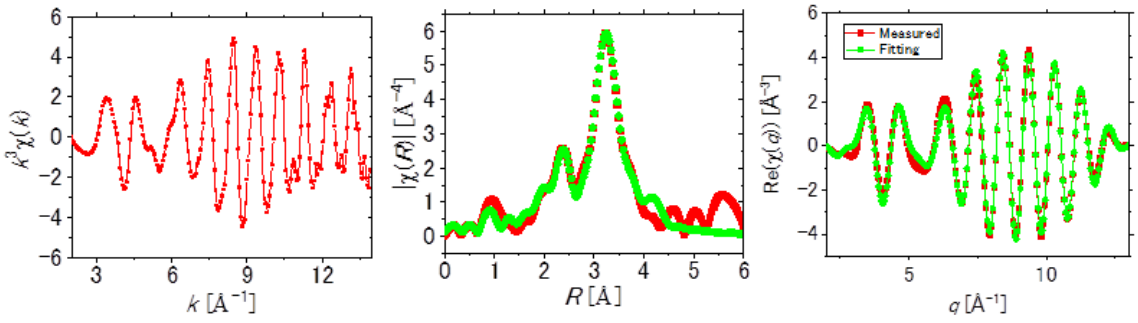

Figure 4. Ba K edge of bulk reference. (A) EXAFS frequency, (B) radial distribution function with fitting for first and second coordination, and (C) real part of inverse Fourier transform of radial distribution function in the range of fitting with R-factor, 0.016.

(A) (B) (C)

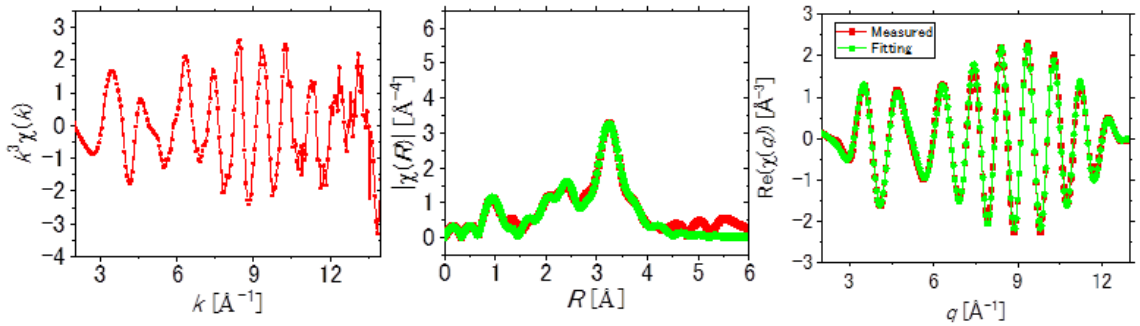

Figure 5. Ba K edge of nanoparticles synthesized in 0.5 s. (A) EXAFS frequency, (B) radial distribution function with fitting for first and second coordination, and (C) real part of inverse Fourier transform of radial distribution function in the range of fitting with R-factor, 0.010.

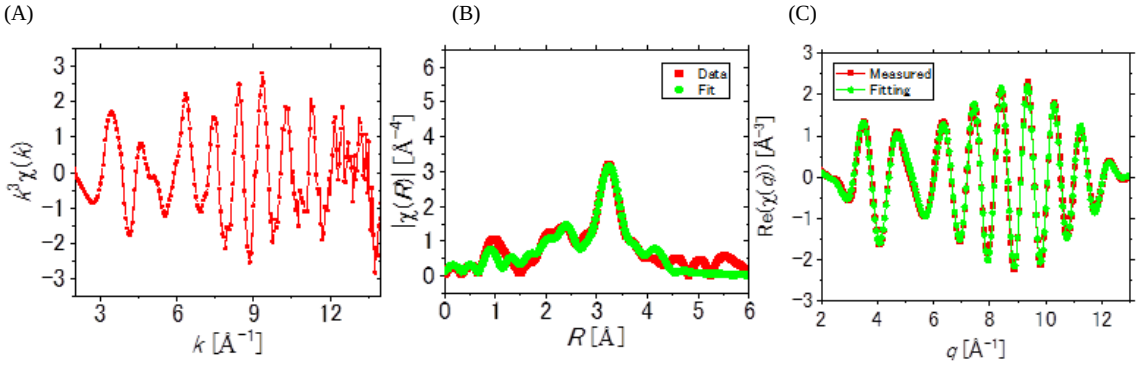

Figure 6. Ba K edge of nanoparticles synthesized in 0.5 s. (A) EXAFS frequency, (B) radial distribution function with fitting for first and second coordination, and (C) real part of inverse Fourier transform of radial distribution function in the range of fitting with R-factor, 0.010.

Figure 7 show time dependence of relative coordination number and Debye-Waller factor of Zr K edge. Relative coordination number was defined with the values of bulk $BaZrO_3$ as a reference. The first coordination numbers were almost constant with residence time whereas that of the second coordination increased significantly. The result is consistent with the TEM-EDX single particle analysis in the previous study [4] suggesting that the Ba uptake in supercritical water with the increase in residence time. The charge was compensated mainly by proton incorporation considering the absence of valence change neither large quantity of oxygen vacancy. On the other hand, as can be seen in Figure 7(B), Debye-Waller factors of nanoparticles were much larger than bulk, and it decreased with increase in residence time. Structural disorder (i.e. atomic displacement) in nanoparticles was large particularly at the initial stage of particle formation, and then it decreased with the incorporation of Ba into the deficient site. The

decrease in atomic displacement was also confirmed by Rietveld analysis for synchrotron X-ray diffraction data.

Figure 8 show time dependence of relative coordination number and Debye-Waller factor of Ba K edge. On the contrary to the local structure around Zr, no significant changes are observed in relative coordination number and Debye-Waller factor whereas Debye-Waller was significantly larger than bulk. These results suggest that the inhomogeneity exists in the single particle, i.e. Ba deficiencies exist in particle surface and the core of the particle forming more ordered perovskite structure with less Ba vacancy. The stability of surface Zr-rich structure than surface Ba-rich structure was confirmed by first-principles calculation for cluster structures.

CONCLUSION

Highly defective structure observed in the $BaZrO_3$ was studied in terms of local structure with EXAFS. As a result, increase in coordination number in the vicinity of Zr and decrease in the Debye-Waller factor with the increase in residence time was detected. The formation of highly defective structure and composition change in supercritical water with reaction time was confirmed by the XAFS analysis. In future, the use of XAFS including *in situ* method would provide new knowledge of nanostructure during the process.

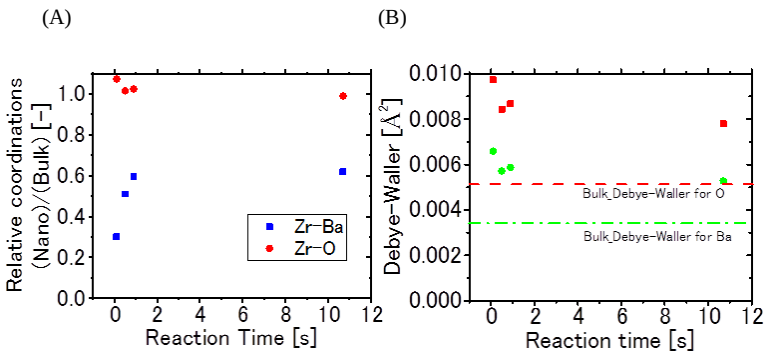

Figure 7. Time dependence of (A) relative coordination numbers and (B) Debye-Waller factor obtained from Zr K edge EXAFS, lines indicate the Debye-Waller factor of bulk.

(A) (B)

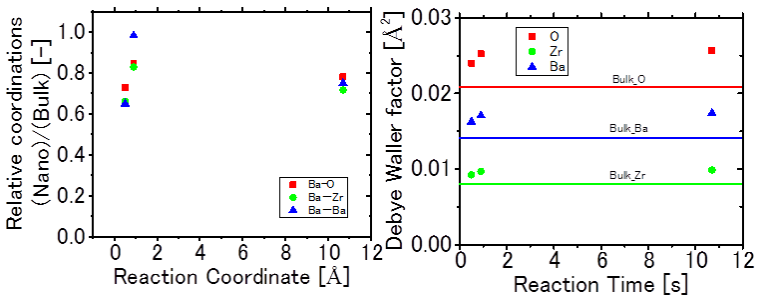

Figure 8. Time dependence of (A) relative coordination numbers and (B) Debye-Waller factor obtained from Zr K edge EXAFS, lines indicate the Debye-Waller factor of bulk.

ACKNOWLEDGEMENTS

The XAFS experiments were performed at the BL01B1, SPring-8, with the approval of the JASRI (Proposal No. 2016A1634).

REFERENCES

[1] T. Adschiri, *et al.*, *Journal of the American Ceramic Society*, **75** (1992) 1019–1022.
[2] A. Yoko, *et al.*, Supercritical hydrothermal synthesis of nanoparticles; in Nanoparticle Technology Handbook (3rd edition), Elsevier, Amsterdam, Application **53** (2018) 683–689.
[3] T. Adschiri and A. Yoko, Supercritical Fluids for Nanotechnology, *The Journal of Supercritical Fluids*, **134** (2018) 167–175.
[4] A. Yoko, *et al.*, *Journal of Nanoparticle Research*, **16** (2014) 1–9.
[5] A. Yoko, *et al.*, *RSC Advances*, **6** (2016) 67525–67533.
[6] A. Yoko, *et al.*, *The Journal of Supercritical Fluids*, **107** (2015) 746–752.
[7] A. Yoko, *et al.*, *Journal of Physical Chemistry C*, **121(22)** (2017) 12220–12229.
[8] S.I. Kawasaki, *et al.*, *The Journal of Supercritical Fluids*, **54** (2010) 96–102.